Published January 13, 2015

Predicting Canopy Temperatures and Infrared Heater Energy Requirements for Warming Field Plots

B. A. Kimball,* J. W. White, M. J. Ottman, G. W. Wall, C. J. Bernacchi, J. Morgan, and D. P. Smith

ABSTRACT

Warming open-field plots using arrays of infrared heaters has proven feasible for conducting experiments to determine the likely effects of global warming on various ecosystems. To date, however, such experiments have been done for only a few degrees (≤3.5°C) of warming, yet climate projections, especially for high latitudes, indicate that future warming may be 10°C or more. Therefore, there is a need to conduct such experiments with more heating, which increases expense. To estimate energy requirements and costs for such temperature free-air controlled enhancement (T-FACE) experiments, improved theory was developed whereby: (i) the canopy temperature of an unheated plot is computed using the well-accepted Monin–Obukhov similarity theory, with some constraints to calculate aerodynamic resistance; (ii) the desired amount of warming is added; and (iii) the energy balance is re-solved to obtain the additional infrared radiation needed from the heaters to attain the desired temperature of the heated plots. Performance data are presented from T-FACE experiments with 3-m-diameter plots conducted over six wheat (*Triticum aestivum* L.) crops and for 1-wk periods over soybean [*Glycine max* (L.) Merr.] and northern mixed-grass prairie. The T-FACE system over wheat provided warming temperatures for day and night that were within 0.1°C of the desired setpoint differences. The measured or predicted energy requirements of the T-FACE system for raising the wheat canopy temperatures averaged about 7.0 kWh m^{-2} d^{-1}. Predictions of canopy temperatures and infrared heating requirements agreed with measurements most of the time for wheat, soybean, and prairie.

Earth continues to warm. The Intergovernmental Panel on Climate Change projects that the global mean surface temperature will rise by 1.1 to 6.4°C by 2100 (Meehl et al., 2007). Moreover, temperature changes in northern ecosystems are projected to be greater than the global mean. For example, by 2100 the temperature increase over Alaska, projected from models forced with the A1B emission scenario, predict maximum increases as high as 11°C (Christensen et al., 2007). The increasing temperatures are likely to affect most organisms, including the processes of soil respiration and sequestration of C, which can add or remove CO_2 from the atmosphere, thereby affecting the degree of warming. Much global change research on biological systems seeks to determine the probable consequences of warming on various organisms and ecosystems. To avoid experimental artifacts, there is a need to conduct such research under conditions as representative as possible of future open fields, i.e., temperature free-air controlled enhancement (T-FACE) experiments.

B.A. Kimball, J.W. White, and G.W. Wall, U.S. Arid-Land Agricultural Research Center, USDA–ARS, 21881 North Cardon Lane, Maricopa, AZ 85138; M.J. Ottman, Plant Sciences Dep., Univ. of Arizona, Tucson, AZ 85721; C.J. Bernacchi, Global Change and Photosynthesis Research Unit, USDA–ARS, 1201 W. Gregory, Urbana, IL 61801; and J. Morgan and D.P. Smith, Crops Research Lab., USDA–ARS, 1701 Center Avenue, Ft. Collins, CO 80526.
Received 26 Feb. 2014. *Corresponding author (Bruce.Kimball@ars.usda.gov).

Published in Agron. J. 107:129–141 (2015)
doi:10.2134/agronj14.0109

One promising approach is to deploy arrays of infrared heaters over experimental plots (e.g., Harte and Shaw, 1995; Nijs et al., 1996; Kimball, 2005, 2011; Kimball et al., 2008). This warming effect is similar to the normal solar heating of leaves, and it is relatively energetically efficient because the leaves are warmed directly without having to overcome a boundary layer resistance, as required if the air were heated first. However, the warming achieved in these initial infrared heating experiments has generally been a modest 3.5°C or less, well below the projected increases for the future.

An equation was derived by Kimball (2005, Eq. [14]) to predict how large an increase in down-welling infrared sky plus heater radiation power is required to produce a unit (1°C) increase in vegetation canopy temperature (T_c) for a unit area of land. Based on weather and plant parameters, the equation predicted the energy requirements of actual heater installations fairly well during daytime conditions but generally underpredicted the heater requirements under calm nighttime conditions (Kimball, 2005; Kimball et al., 2008). However, an 11°C increase in T_c, such as the maximum increase in air temperature projected for Alaska with the A1B emission scenario (Christensen et al., 2007), is beyond "incremental". Therefore the equation merits re-examination.

During the course of analyzing data for this study, we discovered that the "textbook" methodology (e.g., Ham, 2005;

Abbreviations: MOST, Monin–Obukhov similarity theory; PAR, photosynthetically active radiation; PHACE, Prairie Heating and Carbon Dioxide Experiment; PID, proportional integral derivative; RMSD, root mean square difference; T-FACE, temperature free-air controlled enhancement.

Prueger and Kustas, 2005) for the initial step, i.e., predicting T_c of an unheated plot, was problematic. In particular, applying Monin–Obukhov similarity theory (MOST) produced T_c values that were unrealistically low at low wind speeds at night, and convergence on a numeric solution was problematic at high wind speeds. Thus, the purposes of this study were (i) to present a reliable methodology to predict T_c across a wide range of weather conditions, (ii) to derive a more general method for predicting the energy requirements for infrared heating of open-field plots that is applicable for greater degrees of warming, and (iii) to test the method against measured data from T-FACE trials.

THEORY

As mentioned above, Kimball (2005) derived an equation to predict the incremental amount of power required to warm an open-field plot with infrared heaters. His derivation involved linearizing radiation and evaporation terms known to be nonlinear, a simplification that limits applicability of the equation to relatively small increases in T_c. In addition, Kimball (2005) treated the aerodynamic resistance, r_a, as a function only of wind speed, thereby ignoring the effects of buoyancy. This is consistent with the fact that the equation underpredicted under calm conditions but did well under more windy conditions (Kimball, 2005; Kimball et al., 2008). Kimball (2005) also used a constant value for canopy resistance (r_c) for daytime and another constant value for nighttime rather than accounting for variations in r_c due to light intensity, temperature, humidity, and CO_2 concentration. It is possible to redo Kimball's analysis to include the derivative of r_a with respect to changes in T_c. This approach can account for changes in atmospheric stability as the difference between T_c and the air temperature (T_a) changes. However, the result would be a considerably more complex equation, albeit mathematically tractable, and the equation could still be expected to be satisfactory only for relatively small increases in T_c and would not accommodate a more variable r_c. A more promising approach is to avoid differentials altogether. This alternative approach would be: first, determine the canopy temperature of a reference plot (T_{cR}), then add the desired degrees of warming to obtain the desired canopy temperature of the heated plot (T_{cH}), and finally, compute how much more down-welling thermal radiation would be required to balance the surface energy flows of the heated plot.

Basic Energy Balance

The energy balance at the Earth's surface is often expressed as

$$R_n = H + E \quad [1]$$

where R_n is the net radiation (W m^{-2}, positive down), H is the sensible heat flux (W m^{-2}, positive up), and E is the latent heat flux (W m^{-2}, positive up). If needed, R_n in Eq. [1] can be replaced by ($R_n - G$), where G is the soil heat flux (W m^{-2}, positive down). With infrared heating, we can expand R_n to

$$R_n = (1-\alpha)R_s + R_a + R_h - R_c \quad [2]$$

where α is the albedo of the vegetation (or soil or snow as appropriate), R_s is the down-welling solar radiation, R_a is the down-welling sky radiation, R_h is the down-welling radiation from infrared heaters, and R_c is the up-welling radiation from the vegetation canopy (or other surface). The value of R_a can be computed from the air temperature (T_a, °C) and air vapor pressure (e_a, kPa) following Prata (1996).

The values of R_c, H, and E can be computed from

$$R_c = \varepsilon_c \sigma (T_c + 273.15)^4 \quad [3]$$

$$H = \frac{\rho c_p (T_c - T_a)}{r_a} \quad [4]$$

$$E = \frac{(\rho c_p / \gamma)(e_c - e_a)}{r_a + r_c} \quad [5]$$

where ε_c is the emissivity of the canopy (0.98 for most plant leaves [Idso et al., 1969]), σ is the Stephan–Boltzmann constant (5.6697×10^{-8} W m^{-2} K^{-4}), ρ is the air density (kg m^{-3}), c_p is the air heat capacity (J kg^{-1} C^{-1}),), γ is the psychrometric constant (kPa °C^{-1}), e_c is the saturation vapor pressure at T_c (kPa), r_a is the aerodynamic resistance (s m^{-1}), and r_c is the canopy resistance to water vapor transport (s m^{-1}). Values of ρ, c_p, γ, and e_a can generally be obtained from weather data following equations given by Ham (2005), as well as e_c for values of T_c. Note that this is essentially a closed-canopy model. Note also that by using Eq. [5] in a recursive scheme, the problems discussed by Lascano and van Bavel (2007) regarding the common linear assumption of the vapor pressure curve are avoided.

Combining Eq. [1–5] results in

$$0 = -(1-\alpha)R_s - R_a - R_h + \varepsilon_c \sigma (T_c + 273.15)^4 + \frac{\rho c_p (T_c - T_a)}{r_a} + \frac{(\rho c_p / \gamma)(e_c - e_a)}{r_a + r_c} \quad [6]$$

The aerodynamic resistance, r_a, can be calculated using the reciprocal of the conductance equation of Ham (2005, Eq. [86]), which is based on the fairly well-accepted MOST:

$$r_a = \frac{1}{u}\frac{1}{k^2}\left[\ln\left(\frac{z-d}{z_{om}}\right) - \Psi_m\right]\left[\ln\left(\frac{z-d}{z_{oh}}\right) - \Psi_h\right] \quad [7]$$

where u is the wind speed (m s^{-1}) at a standard reference height z (m); k is von Kármán's constant (0.40); d is the zero-plane displacement height (m); z_{om} and z_{oh} are roughness lengths associated with momentum and heat transfer (m), respectively; and Ψ_m and Ψ_h are atmospheric stability or buoyancy correction factors for momentum and heat, respectively. Equations from Monteith (1973) can be used to estimate d and z_{om} from the canopy height, h_c (m): $d = 0.63h_c$ and $z_{om} = 0.13h_c$. Following Prueger and Kustas (2005), $z_{oh} \approx z_{om}/7.4$.

The formulations for the Ψ stability factors are different for stable and unstable atmospheric conditions (Ham, 2005). The stability is described by the Monin–Obukhov length ($L < 0$: unstable; $L > 0$: stable), where

$$L = \frac{-u^{*3}\,\Theta_a \rho c_p}{kgH_v} \quad [8]$$

where u^* is the friction velocity (m s^{-1}) = $uk/\{\ln[(z-d)/z_{om}] - \Psi_m\}$, Θ_a is the absolute air temperature (K), g is the acceleration due to gravity (m s^{-2}), and H_v is the virtual heat flux calculated from $H_v = H + 0.61T_a c_p E$. The formulations for Ψ are

$$\Psi_m = \Psi_h = -5\frac{z}{L} \qquad \text{for } \frac{z}{L} \geq 0 \text{ (stable)} \quad [9a]$$

$$\Psi_m = 2\ln\left(\frac{1+x}{2}\right) + \ln\left(\frac{1+x^2}{2}\right) - 2\arctan(x) + \frac{\pi}{2} \qquad \text{for } \frac{z}{L} < 0 \text{ (unstable)} \quad [9b]$$

$$\Psi_h = 2\ln\left(\frac{1+x^2}{2}\right) \qquad \text{for } \frac{z}{L} < 0 \text{ (unstable)} \quad [9c]$$

where $x = [1 - 16(z/L)]^{1/4}$.

The canopy resistance, r_c, depends on the stomatal conductance g_s (mol m^{-2} s^{-1}) of the leaves as well as on the canopy architecture. For example, for a "standard" 0.5-m-tall alfalfa (*Medicago sativa* L.) crop, r_c = 30 s m^{-1} during the daytime and 200 s m^{-1} at night (Allen et al., 2005), which are the values used by Kimball (2005). However, besides light, the temperature, humidity, and CO_2 concentration are also known to affect g_s, which can be described by the Ball–Berry model (Collatz et al., 1991). This model for stomatal conductance has been criticized for not representing temperature and humidity effects properly (Aphalo and Jarvis, 1993), but it appears to handle light intensity and CO_2 concentration well and is widely used:

$$g_s = m\left(\frac{A_n h_s}{c_s}\right) + b \quad [10]$$

where m (dimensionless) and b (mol m^{-2} s^{-1}) are the slope and intercept constants, respectively, generally obtained by gas exchange measurements from leaf cuvettes, A_n is the net rate of assimilation or CO_2 uptake (μmol m^{-2} s^{-1}), h_s is the relative humidity at the leaf surface (dimensionless), and c_s is the mole fraction of CO_2 at the leaf surface (μmol mol^{-1}).

However, A_n is not readily available, and its computation is complex. Campbell and Norman (1998, Fig. 14.5–14.6) presented curves showing how A_n varies with Q (photosynthetically active radiation, PAR [μmol m^{-2} s^{-1}]) and temperature for a typical C_3 plant. These curves define a response surface that was digitized into a look-up table. Values of solar radiation (W m^{-2}) were converted to Q by multiplying by a factor of 2.0. Sun angle equations from Ham (2005), Duffie and Beckman (1974), Sellers (1965), and Kimball (1973) were used to calculate extraterrestrial solar radiation on a plane parallel to the Earth's surface, $R_{s,ex}$ (W m^{-2}), from latitude, longitude, and time information, as well as the ratio of measured to extraterrestrial radiation, R_{ratio} = $R_{s,meas}/R_{s,ex}$. Then, following Ham (2005) and Spitters et al. (1986), the amount of diffuse radiation, R_{diff}, was calculated from

$$\begin{aligned} R_{diff} &= R_{s,meas} && \text{if } R_{ratio} \leq 0.22 \\ R_{diff} &= R_{s,meas}\left[1.0 - 6.4\left(R_{ratio} - 0.22\right)^2\right] && \text{if } 0.22 < R_{ratio} \leq 0.35 \\ R_{diff} &= R_{s,meas}\left(1.47 - 1.66R_{ratio}\right) && \text{if } 0.35 < R_{ratio} \leq \kappa \\ R_{diff} &= R_{s,meas}\upsilon && \text{if } \kappa < R_{ratio} \end{aligned} \quad [11]$$

where $\upsilon = 0.847 - 1.61\sin(\varepsilon) + 1.04\sin^2(\varepsilon)$, ε is the solar elevation angle (radians), and $\kappa = (1.47 - \upsilon)/1.66$. The amount of direct solar beam radiation, R_{beam}, was calculated from

$$R_{beam} = R_{s,meas} - R_{diff} \quad [12]$$

The extinction coefficient for diffuse solar radiation, K_{diff}, was calculated from

$$K_{diff} = 0.8137 + 0.1042\ln(\chi) + \left[-0.1594 + 0.0897\ln(\chi)\right]\log_{10}(L_t) + \left[-0.0257 + 0.0135\ln(\chi)\right]\left[\log_{10}(L_t)\right]^2 \quad [13]$$

which is an equation fitted to the curves in Campbell and Norman (1998, Fig. 15.4), where L_t is the total leaf area index (m^2 leaf m^{-2} soil), and χ is a leaf area distribution parameter with a value of 1.54 for alfalfa (lucerne in Campbell and Norman, 1998, Table 15.1). This 1.54 value was used for all crops without adjustment. The L_t for an alfalfa crop was calculated from $L_t = 5.5 + 1.5\ln(h_c)$ from Allen et al. (2005).

The extinction coefficient for direct beam solar radiation, K_{beam}, was calculated from Campbell and Norman (1998, Eq. [15.4]):

$$K_{beam} = \frac{\sqrt{\chi^2 + \tan^2(\omega)}}{\chi + 1.774(\chi + 1.182)^{-0.733}} \quad [14]$$

where ω is the solar zenith angle.

Following Campbell and Norman (1998), the average exponentially weighted diffuse flux of PAR was calculated from

$$Q_{diff,avg} = \frac{Q_{diff}\left[1 - \exp\left(-L_t K_{diff}\sqrt{\alpha}\right)\right]}{L_t K_{diff}\sqrt{\alpha}} \quad [15]$$

where α is absorptivity of the leaves, taken as 0.8.

The uninterrupted beam PAR flux, Q_{beam}, was computed from

$$Q_{beam} = Q_o \exp\left(-K_{beam}L_t\right) \quad [16]$$

where Q_o is the PAR flux at the top of the canopy.

The uninterrupted beam plus down-scattered PAR flux, $Q_{beam,t}$, was computed from

$$Q_{\text{beam,t}} = Q_{\text{o}} \exp\left(-K_{\text{beam}} L_{\text{t}} \sqrt{\alpha}\right) \quad [17]$$

and then the scattered beam radiation, $Q_{\text{sc}} = Q_{\text{beam,t}} - Q_{\text{beam}}$.

The PAR flux density absorbed by shaded leaves, Q_{sh}, was

$$Q_{\text{sh}} = \alpha\left(Q_{\text{diff,avg}} + \frac{Q_{\text{sc}}}{2}\right) \quad [18]$$

and by the sunlit leaves, Q_{sl}, was

$$Q_{\text{sl}} = \alpha K_{\text{beam}} Q_{\text{o}} + Q_{\text{sh}} \quad [19]$$

Using Eq. [19] and [18], sunlit and shaded values of A_{n} were obtained from the look-up table for use in Eq. [10].

The sunlit leaf area L_{sl} was computed from

$$L_{\text{sl}} = \frac{1 - \exp\left(-K_{\text{beam}} L_{\text{t}}\right)}{K_{\text{beam}}} \quad [20]$$

and then the shaded leaf area as $L_{\text{sh}} = L_{\text{t}} - L_{\text{sl}}$.

Referring back to Eq. [5], the vapor pressure at the leaf surface, e_{s}, was calculated from

$$e_{\text{s}} = e_{\text{a}} + \frac{E r_{\text{a}} \gamma}{\rho c_{\text{p}}} \quad [21]$$

from which the relative humidity at the leaf surface was then obtained:

$$h_{\text{s}} = \frac{e_{\text{s}}}{e_{\text{s}}^*} \quad [22]$$

where e_{s}^* is the saturation vapor pressure at the leaf temperature, for which T_{c} was used.

Similarly, the CO_2 concentration at the leaf surface was calculated from

$$c_{\text{s}} = c_{\text{a}} - \frac{A_{\text{n}} R T_{\text{c}} r_{\text{a}}}{P} \quad [23]$$

where c_{a} is the CO_2 concentration of the air above the crop, R is the universal gas constant (0.0083144 (kPa m^3 mol^{-1} K^{-1}) and P is the barometric pressure (kPa).

Following Blonquist et al. (2009), Eq. [10] was applied separately to the sunlit and shaded leaf fractions, and then a weighted canopy conductance, g_{c} (mol m^{-2} s^{-1}), was calculated as

$$g_{\text{c}} = g_{\text{s,sun}} L_{\text{sl}} + g_{\text{s,shade}} L_{\text{sh}} \quad [24]$$

from which canopy resistance, r_{c}, was calculated:

$$r_{\text{c}} = \frac{P}{g_{\text{c}} R\left(T_{\text{c}} + 273.15\right)} \quad [25]$$

The values for m and b in Eq. [10] used by Blonquist et al. (2009) were 9.0 and 0.01, respectively. However, we found that the resultant values of r_{c} from Eq. [25] were rather high compared with a robust value of 30 s m^{-1} from Allen et al. (2005) for the daytime r_{c} of a "standard" 0.5-m-tall alfalfa stand. Therefore, we used a value of 17.0 for m, which resulted in an average daytime value of about 30 s m^{-1}. Additional analysis of the wheat data obtained by Wall et al. (2011) yielded a value of 13 for m, which is closer to 17 than the 9.0 of Blonquist et al. (2009). At night for unstressed alfalfa, the value of r_{c} was taken as 200 s m^{-1} following Allen et al. (2005).

The daytime r_{c} in Eq. [25] and the nighttime value of 200 s m^{-1} from Allen et al. (2005) are for a no-stress condition, whereby even at night there can be evaporation from the soil surface even if the stomates are closed. An ability to have stomatal closure with stress was implemented. For every time step, a value of S was input, where $S = 0.0$ gives no stress, and then going linearly up to $S = 1.0$ for which r_{c} is set equal to $r_{\text{c,max}}$, a maximum value of r_{c} corresponding to stomatal closure and dry soil. We used 2000 s m^{-1}.

The interdependence among Eq. [1–25] necessitates an iterative scheme to solve for T_{c}. A scheme that appears to work well most of the time is a variation of the "bisection method" (e.g., Kaw and Kalu, 2008). We first assume that $T_{\text{c}} = T_{\text{a}}$ and compute the difference from zero of Eq. [6]. Then the T_{c} guess is changed by 1.0°C, and the difference from zero in Eq. [6] is again computed. If the difference has the same sign as the previous value, the T_{c} guess is changed by another 1.0°C in the same direction to make the difference from zero smaller. However, if the difference changes sign, the next T_{c} guess is −0.1 times the previous step and the process is repeated. When the sign changes again, the step becomes −0.1 times the previous step, and so on to convergence, hopefully without divergence, oscillation, local minima, or other problems. The criteria used to assure convergence were that the absolute value of the sum of terms on the right side of Eq. [6] was <0.0001 W m^{-2}, or that from one iteration to the next the change in absolute value of the sum was <0.00001 W m^{-2}, or that the absolute value of the difference between estimates of T_{c} from one iteration to the next had to be <0.00001°C. In addition, the absolute value of the changes in estimates of sensible heat, latent heat, and net radiation all had to be <0.0001 W m^{-2}. A case was judged non-convergent when the number of iterations exceeded 9999.

However, during the course of analyzing our data, we encountered problems that led us to use another formulation for r_{a}. Following Jackson et al. (1987), Kimball et al. (1994, 1999), and Bernacchi et al.(2007),

$$r_{\text{a}} = \frac{1}{u}\left[\frac{1}{k}\ln\left(\frac{z - d + z_{\text{o}}}{z_{\text{o}}}\right)\right]^2 \Phi \quad [26]$$

where Φ is a stability or buoyancy correction. The stability correction can be estimated following Mahrt and Ek (1984):

For stable conditions when $T_{\text{c}} < T_{\text{a}}$,

$$\Phi = \left(1 + 15\text{Ri}\right)\left(1 + 5\text{Ri}\right)^{1/2} \quad [27a]$$

For unstable conditions where $T_{\text{c}} > T_{\text{a}}$,

$$\Phi = \left[1 - \frac{15\text{Ri}}{1 + K\left(-\text{Ri}\right)^{1/2}}\right]^{-1} \quad [27b]$$

where Ri is the Richardson number = $g(T_{\text{a}} - T_{\text{c}})(z - d)/(\Theta_{\text{a}} u^2)$, and $K = 75k^2[(z - d + z_{\text{o}})/z_{\text{o}}]^{1/2}/\{\ln[(z - d + z_{\text{o}})/z_{\text{o}}]\}^2$.

Under calm conditions as $u \rightarrow 0$ in Eq. [7] and [26], $r_a \rightarrow \infty$, which leads to predictions of unrealistically cold or hot canopy temperatures. Under such calm conditions, natural convection is the primary mechanism for sensible heat transfer, and for an infinite plane, the American Society of Heating, Refrigerating, and Air-Conditioning Engineers (1972, p. 40) gave the following equation:

$$r_a = \rho c_p \left(\eta \left| T_c - T_a \right|^{1/3} \right)^{-1} \quad [28]$$

where $\eta = 1.52$ and $|T_c - T_a|$ is the absolute value of the temperature difference between canopy and air. In practice, we found that under very calm, stable conditions at night, predicted canopy temperatures that were calculated using Eq. [28] with $\eta = 1.52$ were often too cold and that changing η to 5.0 gave a better fit. In the case when both $u \rightarrow 0$ and $|T_c - T_a| \rightarrow 0$, all three equations (Eq. [7], [26], and [28]) become undefined. For this rare case, we used

$$r_a = \frac{\rho c_p}{2.32} \quad [29]$$

which is equivalent to $|T_c - T_a| = 0.1$°C with $\eta = 5.0$ in Eq. [28].

Calculating Infrared Heater Requirements

As mentioned above, the first step in determining infrared heater requirements is to calculate the canopy temperature of the reference plot, T_{cR}, from weather and vegetation canopy parameters by solving Eq. [1–29] with R_h set at zero. The second step simply is to set the temperature of the heated plot, T_{cH}, equal to $T_{cR} + \Delta T$, where ΔT is the desired degree of warming (°C).

The third step is to compute how much more down-welling thermal radiation from infrared heaters, R_h, would be required to balance the surface energy flows of the heated plot with T_c set to T_{cH} in Eq. [6]. However, even though R_h is a linear term by itself, because of the interdependence of r_a and H when using MOST, an iterative solution is again required. Because T_{cH} is known, the Richardson number can be computed, and then the Mahrt and Ek (1984) formulation (Eq. [26–27]) can be used to estimate an initial value for r_a. An initial estimate for R_h can then be obtained from Eq. [6] to start the iteration for MOST.

In our computations, we again used a variation of the bisection method, using steps of 10 W m^{-2}. The difference from zero in Eq. [6] was then computed. If it was the same sign, the R_h guess was changed by another 10 W m^{-2} in the same direction to make the difference from zero smaller. However, if the difference changed sign, the next R_h guess was −0.1 times the previous step, and the process was repeated. When the sign changed again, the step became −0.1 times the previous step, and so on to convergence, hopefully without oscillation, local minima, or other issues leading to non-convergence. The criteria used to assure convergence were that the absolute value of the sum of terms on the right side of Eq. [6] had to be <0.1 W m^{-2}, the absolute value of the change from one iteration to the next had to be <0.01 W m^{-2}, and the absolute value of the change in estimates of sensible heat, latent heat, and net radiation all had to be <0.1 W m^{-2}. A particular case was judged non-convergent when the number of iterations exceeded 1000.

If the R_h calculated from Eq. [6] with a fixed T_{cH} exceeds the capacity of the infrared heater array, then the down-welling heater radiation will be R_L, the limiting value of the array. In this case, a fourth step is required. The R_h in Eq. [6] is set equal to R_L, and then Eq. [1–29] are iteratively re-solved for T_{cL}, the canopy temperature for the heater-capacity-limited condition.

MATERIALS AND METHODS

Experimental data on the performance of T-FACE systems consisting of hexagonal infrared heater arrays like those described by Kimball et al. (2008) were obtained for wheat, soybean, and northern mixed-grass prairie. The wheat data were obtained from a Hot Serial Cereal experiment conducted at Maricopa, AZ, as described in more detail by Wall et al. (2011, 2013), Ottman et al. (2012), Kimball et al. (2012), and White et al. (2011, 2012). Briefly, wheat (the "Cereal") was planted approximately every 6 wk ("Serially") for 2 yr starting in March 2007. For six of the plantings (early fall, midwinter, and spring), infrared heater arrays ("Hot") were deployed in a Latin square experimental design with three replicates each of heated plots, reference plots with dummy heaters, and control plots with no experimental apparatus. As described by Kimball et al. (2008), the plots were 3 m in diameter and were located in the center of 11-m-square blocks of wheat. Calibrated infrared thermometers (Model IRR-PN, Apogee Instruments Inc.) were used to sense canopy temperatures in the heated and reference plots. The canopy temperature data were processed by dataloggers (Models CR7 and CR23X, Campbell Scientific) equipped with current/voltage output modules (Model SDM-CV04, Campbell Scientific), which provided 0- to 10-V control signals to dimmers (Model LCED-2484, 240V, 35A; Kalglo Electronics Co., Inc.). The dimmers, in turn, modulated the output of the heaters (Model FTE-1000 [1000 W, 240 V, 245 mm long by 60 mm wide] mounted in reflector housings [Model ALEX-F (254 mm long by 98.6 mm wide by 89.4 mm high)], Mor Electric Heating Associated Inc.) so as to maintain the canopy temperature of the heated plots at 1.5°C warmer than the reference plots during daytime and 3.0°C warmer at night.

During the Hot Serial Cereal experiment, solar radiation, air temperature, and wind speed were measured on a weather mast in the experimental field most of the time starting with the fall 2007 planting. For times when field mast data were not available, we utilized data from the AZMET weather station (http://ag.arizona.edu/AZMET/) located about 1 km away. A bias between air temperatures measured at the field and by AZMET was detected when data from times when both were operating were plotted against each other. Consequently, AZMET data were adjusted to the field condition using a regression equation that had solar radiation and wind speed as covariates. Wind speeds measured at the field mast at the 2-m height were adjusted upward to the 3-m height of AZMET following Ham (2005) and using the canopy height for the wheat in the central plot where the field mast was located.

Similar T-FACE arrays were deployed over 3-m-diameter subplots within the larger 18-m-diameter CO_2–FACE plots of soybean in the SoyFACE Project at Urbana, IL, for the summer 2009 growing season. Details of the SoyFACE Project with the T-FACE subplots were described by Ruiz-Vera et al. (2013),

although the data used in this study came from only one plot at ambient CO_2. A big difference from Hot Serial Cereal is that, unlike using six single 1000-W heaters in a hexagonal array as described by Kimball et al. (2008), SoyFACE used 24 heaters (FTE-1000, 1000W, 240V, 245 mm long by 60 mm wide, Mor Electric Heating Association Inc.), which were mounted in six groups of four heaters in ALEX-FFFF reflector housings (also from Mor) and arranged in a hexagonal pattern. The setpoint temperature difference was 3.5°C night and day in SoyFACE.

Data were also obtained from the Prairie Heating and CO_2 Experiment (PHACE) at Cheyenne, WY, on northern mixed-grass prairie vegetation. This experiment and its T-FACE arrays were described previously by Kimball et al. (2008) and Morgan et al. (2011). Like the Hot Serial Cereal experiment, the setpoint temperature differences were 1.5 and 3.0°C during day and night, respectively.

Canopy temperature data from heated and reference plots for all three experiments (Hot Serial Cereal, SoyFACE, and PHACE) were corrected for reflected sky radiation as follows. The radiation, R_I, sensed by the infrared thermometers (IRTs), which had an 8- to14-μm wavelength window (Apogee Instruments) can be written as

$$R_I = (1-\varepsilon_c)R_{a8} + f_{8c}R_c \quad [30]$$

where R_{a8} is the sky radiation in the 8- to 14-μm band, f_{8c} is the fraction of the total radiation emitted from the canopy (i.e., $\varepsilon_c\sigma\Theta_c^4$) in the 8- to 14-μm band, and ε_c is the emissivity of the canopy (taken as 0.98 for all three canopy types). The IRTs were calibrated using a black-body source, and the internal electronics interpret R_I to give an apparent temperature, Θ_I (K), of the target canopy such that

$$R_I = f_{8I}\sigma\Theta_I^4 \quad [31]$$

where f_{8I} is the fraction of black-body radiation (i.e., $\sigma\Theta_I^4$) in the 8- to 14-μm band. The canopy radiation, R_c, at absolute canopy temperature Θ_c (K) is

$$R_c = \varepsilon_c\sigma\Theta_c^4 \quad [32]$$

Similarly, the sky radiation can be written as

$$R_{a8} = \varepsilon_{a8}\sigma\Theta_a^4 \quad [33]$$

where ε_{a8} is the effective hemispherical emissivity of the sky in the 8- to 14-μm band and Θ_a (K) is the screen-level absolute air temperature. The sky emissivity in the 8- to 14-μm band in the zenith direction, ε_{a8z}, was calculated from an equation created by Idso (1981b):

$$\varepsilon_{a8z} = 0.24 + \left(2.98\times10^{-6}\right)e_a^2\exp\left(\frac{3000}{\Theta_a}\right) \quad [34]$$

where e_a is the screen-level vapor pressure (kPa). Idso (1981a) also derived a correction to convert zenith to hemispherical emissivity:

$$\varepsilon_{a8} = \varepsilon_{a8z}\left(1.4 - 0.4\varepsilon_{a8z}\right) \quad [35]$$

The fraction of black-body radiation in the 8- to 14-μm band emitted at temperature Θ_I was computed from (Kimball et al., 1982)

$$f_{8I} = -0.6732 + \left(0.6240\times10^{-2}\right)\Theta_I - \left(0.9140\times10^{-5}\right)\Theta_I^2 \quad [36]$$

Because Θ_c is quite close to Θ_I, f_{8c} is very close to f_{8I}, so they were equated.

Therefore, using values calculated from Eq. [34], [35], and [36], substituting Eq. [31], [32], and [33] into Eq. [30], and rearranging to solve for the true canopy temperature, Θ_c (K), yields

$$\Theta_c = \left\{\frac{1}{\varepsilon_c}\left[\Theta_I^4 - \frac{(1-\varepsilon_c)\varepsilon_{a8}\Theta_a^4}{f_{8I}}\right]\right\}^{1/4} \quad [37]$$

Following Kimball et al. (2008), a procedure similar to these steps was used in real time by the dataloggers in all three experiments to correct the T_{cH} of the heated plots for radiation emitted from the heaters in the 8- to 14-μm band and reflected from the plant canopies.

The electrical power per heated plot (Z, W m^{-2}) consumed by the heaters in all three experiments was calculated from

$$Z = \frac{\text{Heat}\left(\text{W plot}^{-1}\right)\left(\text{PID Volts}/10\text{ V max.}\right)^2}{7.07\text{ m}^2\text{ plot}^{-1}} \quad [38]$$

where PID Volts is the proportional-integral-derivative control signal sent from the dataloggers to the dimmers to modulate heater output. Equation [38] assumes that the alternating current (AC) voltage output from the dimmers is linearly proportional to the direct current (DC) voltage signal sent to the dimmers. The squared term in parentheses is squared because power consumption is related to the square of the voltage supplied to the heaters. For the Hot Serial Cereal and PHACE experiments, the heater watts per plot was 6000, and for SoyFACE, it was 24,000. To minimize damage to the heaters due to water-caused short circuits, the dataloggers in the SoyFACE Project were programmed to send no less than 2.5 V to the dimmers, which meant that they should have operated at no less than 1/8 maximum power. This precaution was not taken in the Hot Serial Cereal or PHACE experiments, so their minimum power consumption was zero.

The infrared radiation impinging on each heated plot from the heaters was linked to electrical power consumption by a wind-dependent efficiency equation determined by Kimball et al. (2008) and Kimball and Conley (2009):

$$\text{Efficiency}(\%) = 10 + 25\exp(-0.17u) \quad [39]$$

where u is wind speed at the 2-m height.

RESULTS AND DISCUSSION

Predicting Canopy Temperatures of Unheated Plots

As alluded to in above, convergence problems were encountered when we attempted to compute canopy temperatures, T_c, from field weather data when using MOST to calculate aerodynamic resistance, r_a (Eq. [7–9]). Therefore, to understand which conditions were likely to cause such convergence problems, we defined a dry night, humid night, dry day, and humid day (Table 1) and made computations across a range of wind speeds, u, from 0.1 to 10.0 m s^{-1} (Fig. 1). The vegetation characteristics were those of a "standard" 0.5-m-tall alfalfa crop (Allen et al., 2005) with a canopy resistance, r_c, of 30 s m^{-1} during daytime and 200 s m^{-1} at night (Table 1). First, under both dry and humid, stressed and unstressed conditions, as u decreased, the T_c predicted using MOST became very cold and unrealistic, as can be inferred from sharp bends toward cold temperatures for the night curves for values of u below about 2 m s^{-1} in Fig. 1c. However, in Fig. 1c, the nighttime curves reached a flat minimum, which were the T_c corresponding to the use of Eq. [28] for r_a under calm conditions and represented the maximum values for the night curves in Fig. 1b. During daytime for both unstressed and stressed conditions, the curves for both T_c (Fig. 1c) and r_a (Fig. 1b) appeared well behaved except at very low (<0.2 m s^{-1}) wind speeds, where there were convergence problems.

Although the curves for T_c (Fig. 1c) and r_a (Fig. 1b) appeared well behaved at high wind speeds, the curves for latent (E) and sensible (H) heat fluxes initially were problematic when using MOST alone. At high wind speeds, small changes in the T_c estimates caused large swings in the two heat flux estimates. Moreover, the method converged on different values for the fluxes depending on the initial values. For example, suppose the computations were initialized with $T_c = T_a$, a neutral temperature profile, and a u of 10 m s^{-1}, and then the iterations were done to obtain the T_c and fluxes for this 10 m s^{-1} case. Next, for a u of 9 m s^{-1}, the initial values were these final numbers from 10 m s^{-1}, and so forth stepping down to slower u to obtain particular curves of E and H vs. u. In contrast, if the computations started with a u of say 3 m s^{-1}, also starting with $T_c = T_a$ and a neutral temperature profile and then stepping to higher u using the final values for the lower speed for the initial values, different curves were obtained. Obviously, there was considerable uncertainly in the values for E and H at higher u using MOST, even if the T_c appeared well behaved.

As already mentioned, we have previously used the Mahrt and Ek (1984) equations (Eq. [26–27]) for calculating r_a, and because they are based on the Richardson number rather than the Monin–Obukhov length for the stability parameter, the iterative procedure to compute canopy temperature is more stable, requiring comparatively few iterations before convergence is achieved. Therefore, we implemented a hybrid procedure whereby T_c and the corresponding energy fluxes were calculated first using the Mahrt and Ek equations, and these values were used as the initial values for MOST. Using this hybrid procedure to obtain r_a and using Eq. [10–25] (i.e., following Campbell and Norman [1998] and Blonquist et al. [2009]) for r_c, curves for T_c, r_a, and the corresponding energy fluxes were computed across a wide range of wind speed (Fig. 1). There was little difference

Table 1. Weather parameters and canopy resistance for alfalfa (Allen et al., 2005) used to define meteorological conditions for a dry night, humid night, dry day, and humid day.

Condition	Air temp.	Air vapor pressure	Relative humidity	Solar radiation	Canopy resistance
	°C	kPa	%	W m^{-2}	s m^{-1}
Dry night	10	0.2	16	0	200
Humid night	10	1.2	98	0	200
Dry day	30	0.2	5	1000	30
Humid day	30	1.2	28	1000	30

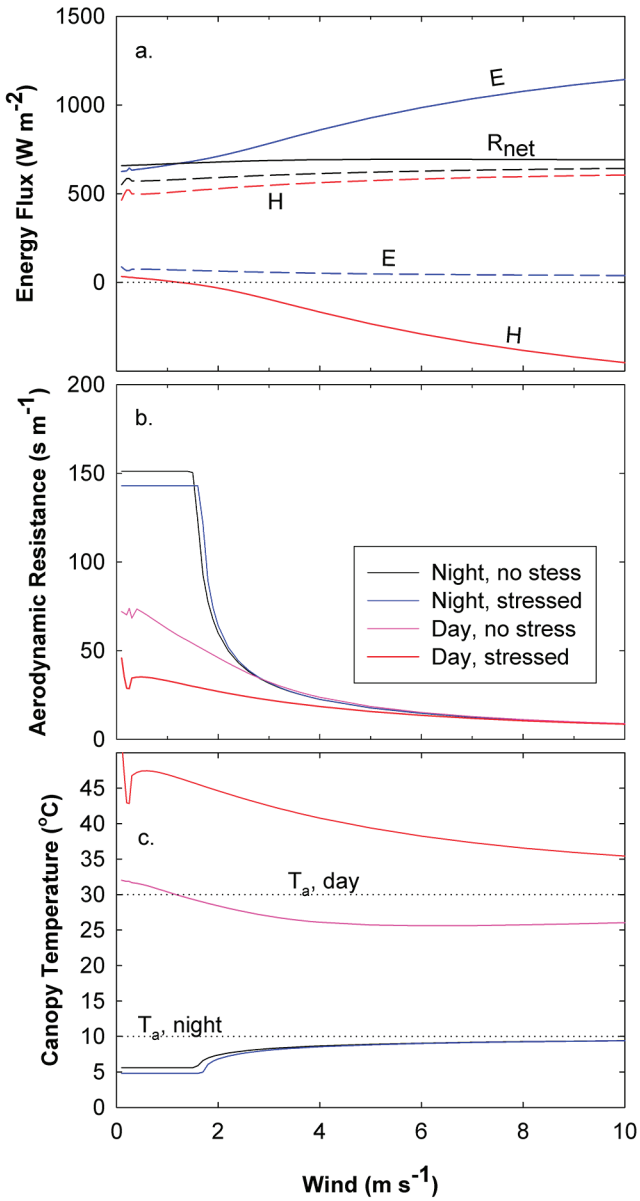

Fig. 1. (a) Net radiation (R_n) and sensible (H), and latent (E) heat fluxes vs. wind speed (u) computed with the hybrid Mahrt–Ek/Monin–Obukhov similarity theory (MOST) procedure for canopy resistance (r_c) on a humid day (Table 1) with no stress (solid lines) and stress (dashed lines) in an unheated reference plot; (b) for aerodynamic resistance (r_a) at night with no stress and stressed and in the day with no stress and stressed; and (c) for canopy temperature (T_c) vs. wind speed at night with no stress and stressed and in the day with no stress and stressed. The vegetation characteristics were those of a "standard" 0.5-m-tall alfalfa crop (Allen et al., 2005).

between the MOST and hybrid curves for T_c at higher u, and at very low u, the hybrid method had smaller changes from one value of u to another. However, compared with MOST alone, the hybrid procedure converged to consistent values at higher u. Whether starting from 10 m s^{-1} and going to slower u or starting from 3 m s^{-1} and going to higher u, the hybrid procedure produced the same curves plotted in Fig. 1a.

The energy fluxes in Fig. 1a vary as expected with increasing u with E under no stress, going from about 600 W m^{-2} at low u to 1200 W m^{-2} at 10 m s^{-1}, and it is near zero under stress. Canopy temperatures during daytime with no stress are above T_a for u below about 1.5 m s^{-1}, but then they dip below T_a by about 4.5°C at u >4 m s^{-1} (Fig. 1c). Under stress during daytime, T_c rises toward about 20°C above T_a as u decreases toward zero, and it is about 5°C above T_a at high values of u.

The ability of the procedure to predict wheat canopy temperatures in the reference plots, T_{cR}, of the Hot Serial Cereal experiment is illustrated in Fig. 2. For these comparisons between observed and predicted wheat (as well as soybean and prairie below) data, the model parameters were those for standard alfalfa as presented above, except that measured values for crop height were used. Although there is more scatter than desired in Fig. 2, the calculated and measured data points fall along the 1:1 lines for five of the six wheat crops, which provides assurance that the method is reliable. Root mean square differences (RMSDs) between measured and predicted T_{cR} values were calculated as

$$\mathrm{RMSD} = \sqrt{\sum\left[\frac{(\mathrm{measured} - \mathrm{predicted})^2}{n}\right]} \qquad [40]$$

where n is the number of pairs of measured and predicted values. The RMSDs are 4.0, 2.6, 7.1, 3.2, 3.3, and 2.4°C for the 13 Mar. 2007, 17 Sept. 2007, 2 Jan. 2008, 10 Mar. 2008, 20 Sept. 2008, and 1 Dec. 2008 plantings, respectively. No data for the September plantings following freezes are included. For reasons we do not understand, the data for the 17 Jan. 2008 planting date are more variable, with an RMSD of 7.1, and the data do not consistently clump along the 1:1 line.

Convergence problems were very minor using the hybrid procedure with the Hot Serial Cereal data. Over 17,559 h for the six crops, convergence for predictions of T_{cH} of the unheated reference plots and of R_h for the heated plots were not achieved for only 11 and 3 h, respectively. Moreover, the values that were computed for those non-convergent hours were generally intermediate to those of the hours just before and just after, so no unrealistic values were ever predicted.

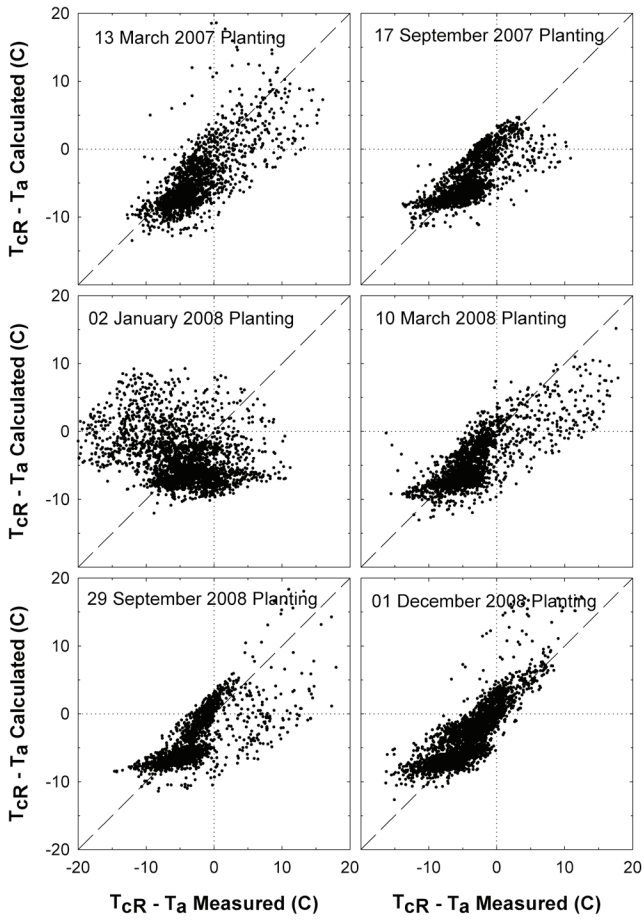

Fig. 2. Values of hourly canopy temperatures for reference plots computed using the hybrid Mahrt–Ek/Monin–Obukhov similarity theory (MOST) method minus air temperature ($T_{cR} - T_a$ calculated) vs. corresponding measured hourly average wheat canopy temperatures minus air temperatures observed in the reference plots ($T_{cR} - T_a$ measured) of six crops with varying planting dates in the Hot Serial Cereal experiment at Maricopa, AZ. The dashed lines are the 1:1 lines.

Predicting Heating Requirements

Using the hybrid Mahrt–Ek/MOST method to obtain r_a and Eq. [11–25] to obtain r_c, the infrared heating requirements to warm a "standard" 0.5-m-tall alfalfa crop by 1°C were computed for an actively growing crop during daytime and night (Fig. 3) and for a stressed crop whose stomates are closed (r_c = 2000 s m^{-1}) during daytime. As expected, much more infrared radiation is required to raise T_c for an actively transpiring crop during daytime compared with one with stomates closed at night or with stomates closed due to stress. Comparing Fig. 3

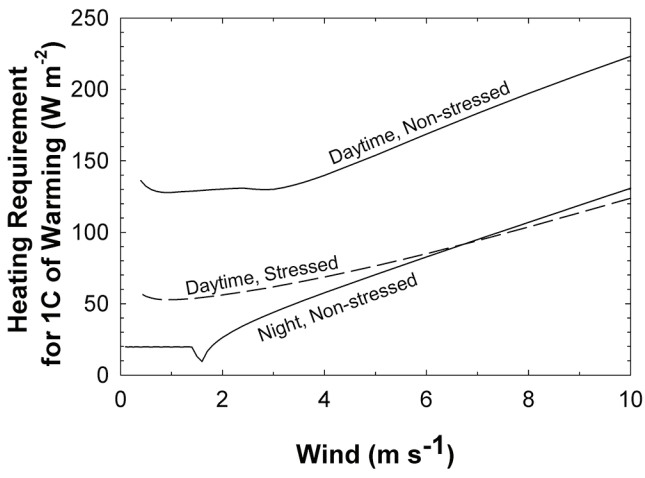

Fig. 3. Infrared heating requirement to warm a standard 0.5-m-tall alfalfa crop (Allen et al., 2005) by 1°C vs. the wind speed for non-stressed vegetation day and night and for vegetation that has closed stomata due to stress. Weather parameters for the computations were those for a humid day and night (Table 1). The hybrid Mahrt–Ek/Monin–Obukhov similarity theory (MOST) procedure was used to calculate aerodynamic resistance. Convergence problems were encountered at wind speeds <0.3 m s^{-1} during the daytime, so these values are not shown.

computed with the more complex procedure presented here with Fig. 7 of Kimball (2005), which was computed using his incremental method, the curve for daytime, unstressed is much higher at low wind speed (i.e., about 130 W m^{-2} compared with 50 W m^{-2} at 1 m s^{-1}).

As discussed above, there is a need to predict infrared heating requirements for experiments that have warming by 10°C and more. Therefore, we computed the heating requirements for a "standard" 0.5-m-tall alfalfa crop (Allen et al., 2005) for 1°C, 10°C, and several points in between for unstressed vegetation, day and night, and for stressed vegetation (stomata closed) during daytime at wind speeds, *u*, of 2 and 8 m s^{-1} (Fig. 4). There is some curvature, with the 2 m s^{-1}, nighttime case curving most. However, the deviation from linearity is small, so the incremental equation of Kimball (2005) would have errors of <10% out to about 5°C of warming.

Measured Performance of the System during the Hot Serial Cereal Experiment

The ability of the T-FACE system to maintain the warming treatment during the Hot Serial Cereal experiment on wheat at Maricopa, AZ, is illustrated in Fig. 5, which shows the histogram of 10-min-average canopy temperature differences between heated and reference plots. The data are from six growing seasons and three replicates within each season. The peaks for both day and nighttime curves are close to our target 1.5 and 3.0°C of warming for day and night, respectively. However, the curves are somewhat skewed to the left (cooler than target) because of the inability of the T-FACE system to maintain the setpoint differences under high-wind conditions. One surprising observation from the Hot Serial Cereal experiment occurred when the early-fall-planted wheat crops in the reference and control plots suffered frost damage at midwinter just when they were close to anthesis (Wall et al., 2011; Ottman et al., 2012), whereas the wheat in the heated plots suffered little damage. As a consequence, evapotranspiration nearly ceased in the reference plots, and they became abnormally warm, such that the T-FACE system could not warm the heated plots by the target 1.5°C above the reference plots during daytime, and these data when the reference plots were frost damaged also caused the histograms in Fig. 1 to be skewed to the left. Nevertheless, the modes of the two curves are on (night) or only 0.1°C below (day) the targets, whereas the average degrees of warming were 1.3 and 2.7°C during day and night, respectively.

The measured energy consumption of the heaters based on hourly average PID control signals sent by the dataloggers to the dimmers averaged across all six growing seasons was about 7.0 kWh m^{-2} d^{-1} (Table 2) when there was no frost damage. The two fall-planted crops (17 Sept. 2007 and 29 Sept. 2008) had the highest average energy consumption at 9.1 kWh m^{-2} d^{-1}, but these values included time periods when the wheat in the reference plots had abnormally high canopy temperatures due to decreased evapotranspiration as a result of frost damage, and therefore the heated plots were being warmed more than they would have if such damage in the reference plots had not happened. Such a lack of a proper reference plot can be a problem with the infrared heater method whenever the warming treatment itself alters the canopy architecture, plant physiology, albedo, etc., in ways that affect the energy balance of the canopy.

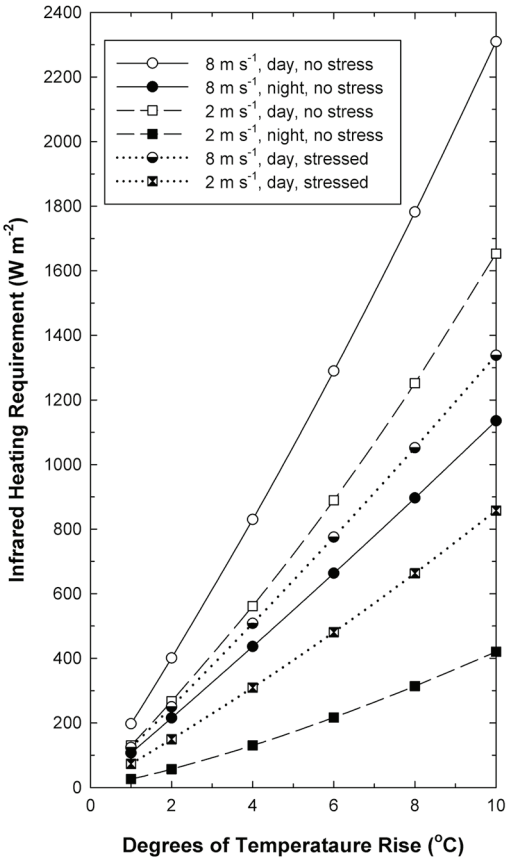

Fig. 4. Infrared heating requirement to warm a standard 0.5-m-tall alfalfa crop (Allen et al., 2005) during daytime and nighttime vs. the temperature rise. Also shown are the heating requirement for a similar alfalfa crop that is stressed (canopy resistance = 2000 s m^{-1}). Weather parameters for the computations were: wind speed = 2.0 and 8 m s^{-1}; air temperature = 30°C during daytime and 10°C at night; air vapor pressure = 1.2 kPa; and solar radiation during daytime = 1000 W m^{-2}. The hybrid Mahrt–Ek/Monin–Obukhov similarity theory (MOST) procedure was used to compute aerodynamic resistance.

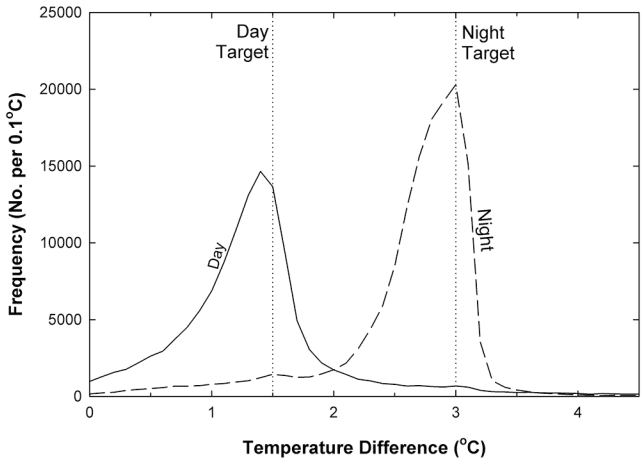

Fig. 5. Frequency distribution of the 10-min-average wheat canopy temperature differences between heated and reference plots from the Hot Serial Cereal experiment at Maricopa, AZ, for day and night separately. Also shown are the daytime and nighttime target setpoint differences (1.5 and 3.0°C, respectively). Data from six growing seasons and three replicate pairs of plots are included. Times of sunrise and sunset are not shown.

Table 2. Infrared heating requirements for six wheat crops in the Hot Serial Cereal experiment at Maricopa, AZ, calculated from readings of the power company's meter for the specified time periods for which unambiguous attributions could be made for the power usage (i.e., no starting or stopping or other tests being done), calculated each hour from the proportional-integral-derivative (PID) control signals sent by the dataloggers to the dimmers that modulated heater output per Eq. [38], and computed from weather data using the hybrid Marhrt–Ek/Monin–Obukhov similarity theory (MOST) procedure to calculate canopy resistance. The power company's meter supplied electricity to the field and also measured the power used by the irrigation pump, the air conditioner/heater for the instrument trailer, and occasional power tools.

Planting date	Time period	Duration	Plots	Heating requirement		
				Power company meter	Measured from PID	Theory
		d	no.	kWh m^{-2} d^{-1}		
13 Mar. 2007	20 Mar. 2007–6 June 2007	78	3		7.4	7.3
17 Sept. 2007	27 Sept. 2007–24 Feb. 2008	151	3		9.1†	5.8
	27 Sept. 2007–25 Dec. 2007	90	3		7.0	5.7
2 Jan. 2008	17 Jan. 2008–12 May 2008	117	3		6.6	6.5
10 Mar. 2008	12 Mar. 2008–12 June 2008	93	3		8.0	7.1
29 Sept. 2008	3 Oct. 2008–2 Mar. 2009	151	3		9.1†	5.9
	3 Oct. 2008–26 Dec. 2008	85	3		6.4	5.6
1 Dec. 2008	5 Dec. 2008–27 Apr. 2009	144	3		6.8	6.2
Avg. without frost days					7.0	6.4
17 Sept. 2007	12 Dec. 2007–11 Jan. 2008	31	3	14.7†	11.3†	5.7
17 Sept. 2007	21 Jan. 2008–22 Feb. 2008	33	6	12.9†	12.0†	6.0
2 Jan. 2008					7.0	1.4
2 Jan. 2008	13 Mar. 2008–12 May 2008	61	6	10.9	6.6	7.7
10 Mar. 2008					7.9	6.6
10 Mar. 2008	17 May 2008–12 June 2008	27	3	11.4	8.3	8.1
29 Sept. 2008	7 Oct. 2008–28 Nov. 2008	53	3	9.5	5.5	5.4
29 Sept. 2008	19 Dec. 2008–2 Mar. 2009	74	6	12.6†	12.5†	6.3
1 Dec. 2008					6.2	5.3
1 Dec. 2008	4 Mar. 2009–27 Apr. 2009	55	3	11.3	8.4	8.1
Weighted avg. for no. of plots and days, no frost				10.7	7.0	6.2
Weighted avg. for no. of plots and days, with frost				13.1	12.1	

† Time periods when the wheat in the reference plots had abnormally high canopy temperatures due to decreased evapotranspiration as a result of frost damage, and therefore the heated plots were being warmed more than they would have if such damage in the reference plots had not happened.

The winter-planted crops (2 Jan. 2008 and 1 Dec. 2008) had lower daily energy consumption (6.6 and 6.8 kWh m^{-2} d^{-1}, respectively) than the spring-planted crops (13 Mar. 2007 and 10 Mar. 2008 had 7.4 and 8.0 kWh m^{-2} d^{-1}, respectively), consistent with overall lower temperatures and lower evapotranspiration rates experienced by the winter-planted crops.

However, the energy consumption determined from the datalogger heater control signals was only about 0.65 of that measured by the electrical power company's wattmeter for time periods when comparisons could be made (Table 2). That there was this much discrepancy between the two methods is surprising because our estimates of average energy consumption by the irrigation pump, for example, would be <0.1 kWh m^{-2} d^{-1} (calculated using the power of the motor multiplied by the time of operation and divided by the heated plot area), and it seems unlikely that energy used by the air conditioner for the trailer, lights, power tools, etc., would have been much more than 0.1 kWh m^{-2} d^{-1}. The control signals varied widely from minute to minute to maintain the target setpoint canopy temperature differences (Fig. 5), so they probably are not as reliable as a wattmeter. On the other hand, the power company's meter was obviously in error during our first crop (13 Mar. 2007 planting), so no data are shown for this crop, and the company replaced the meter during the 2007 summer. They replaced this second meter with a third one about a year later with no explanation. Thus, the power company data are somewhat suspect as well.

Predicted Infrared Heater Power Requirements of the System during the Hot Serial Cereal Experiment

Using the procedure presented here with the hybrid Mahrt–Ek/MOST method for r_a and Eq. [11–25] for r_c, and assuming no stress, the hourly electrical energy requirements were calculated from hourly weather data. The infrared heater electrical power requirements calculated from theory averaged 6.4 kWh m^{-2} d^{-1}, which was slightly smaller (9% on average) than that determined from the PID control signals sent from the dataloggers to the dimmers (Table 2). This agreement gives some assurance that the theory is accurate. However, the fact that that both the theory and PID-determined values were about two-thirds of that from the power company's wattmeters introduces uncertainty.

Comparative Performance of the Arrays in the Experiments

The weather conditions were quite different for selected week-long data sets from the Hot Serial Cereal (HSC), SoyFACE, and PHACE experiments (Fig. 6a, 6e, and 6i). Especially noteworthy are the higher vapor pressures for SoyFACE and the higher wind speeds for PHACE compared with the other two locations.

The predicted and measured canopy temperatures, T_c, agreed well for HSC and SoyFACE (Fig. 6b and 6f; RMSDs of 2.0 and 2.5°C, respectively, Table 3), but measured values tended to be higher for PHACE at night (Fig. 6j; RMSD of 4.7°C, Table 3). Most of the time, the T-FACE systems were able to maintain the

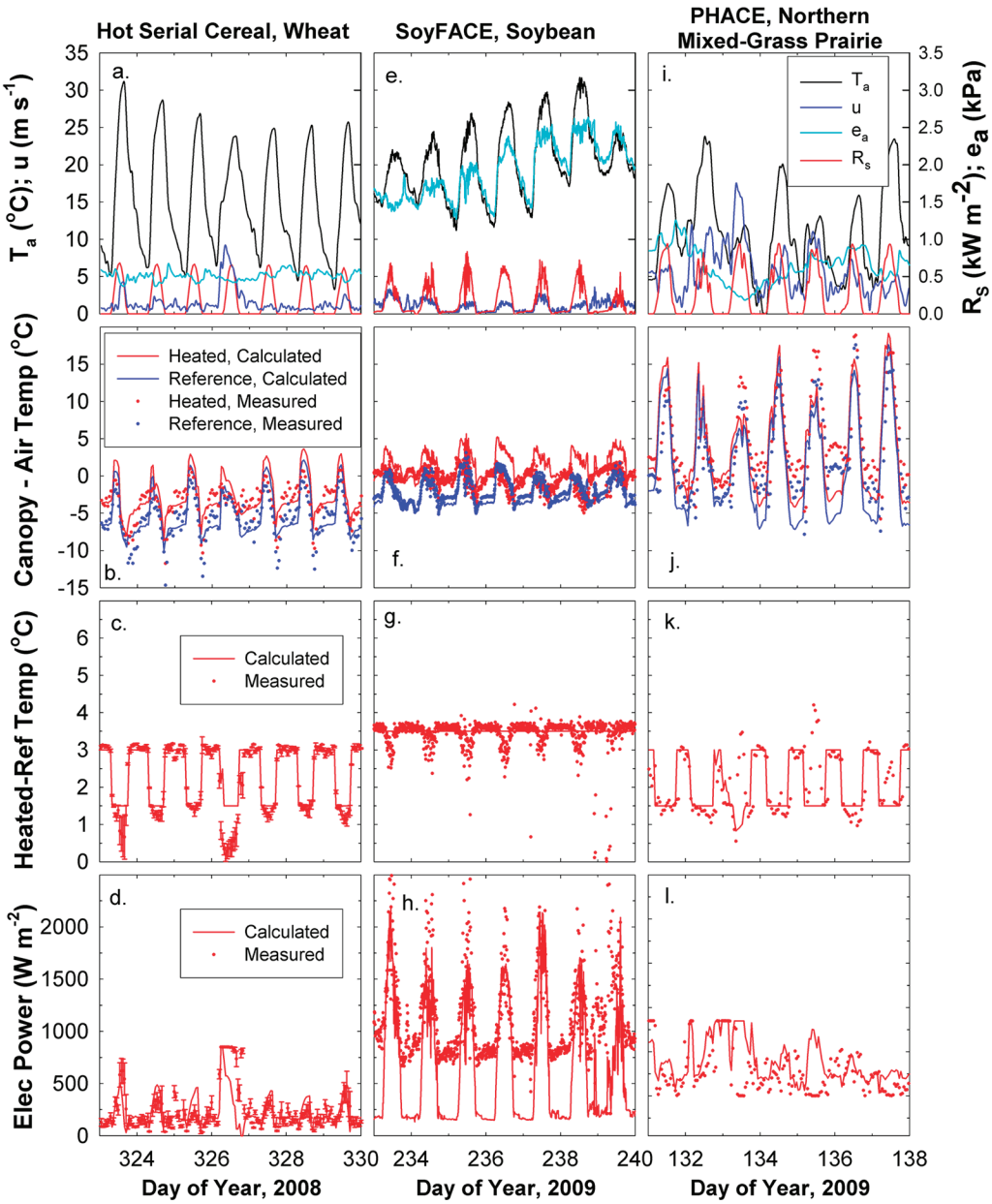

Fig. 6. Air temperature (T_a), wind speed (u), water vapor pressure (e_a), and solar radiation (R_s) for 1 wk each from (a) the Hot Serial Cereal (HSC) experiment at Maricopa, AZ, for wheat, (e) the SoyFACE Project at Urbana, IL, for soybean, and (i) the PHACE Project at Cheyenne, WY, for northern mixed-grass prairie; (b,f,j) measured and calculated canopy temperatures minus corresponding air temperature for heated and reference plots in HSC, SoyFACE, and PHACE, respectively; (c,g,k) measured and calculated canopy temperature differences between the heated and corresponding reference plots for HSC, SoyFACE, and PHACE, respectively; and (d,h,l) measured and calculated electric power consumption for warming the heated plots in HSC, SoyFACE, and PHACE, respectively. The hybrid Mahrt–Ek/Monin–Obukhov similarity theory (MOST) procedure was used to calculate aerodynamic resistance. The minimum electric power consumption was taken as zero for HSC and PHACE and as 407 W m^{-2} for SoyFACE. The setpoint temperature differences were 1.5 and 3.0°C for day and night, respectively, for HSC and PHACE and a constant 3.5°C for SoyFACE.

desired setpoint increases of the heated plots above the reference plots ($T_{cH} - T_{cR}$), and the predicted increases are close to the measured increases for all three experiments (Fig. 6c, 6g, and 6k; RMSDs of 0.4, 0.5, and 0.8°C, respectively, Table 3). The largest deviations occurred near noon on the first and fourth days depicted for the HSC experiment, when the T-FACE system failed to raise the T_c to the desired setpoint difference, yet the predictions indicate it should have been able to do so.

The electrical power requirements were higher for the PHACE experiment than the HSC experiment (Fig. 6l vs. 6d), consistent with the higher wind speeds at Cheyenne, WY. The measured power usage for SoyFACE was higher than predicted,

Table 3. Root mean square differences between observed and measured canopy temperatures of the reference plots (T_{cR}) and of the heated plots (T_{cH}) and of their differences ($T_{cH} - T_{cR}$), as well as of the electrical power consumption (Z) for the Hot Serial Cereal (wheat), SoyFACE (soybean), and PHACE (northern mixed-grass prairie) data plotted in Fig. 6.

Parameter	Hot Serial Cereal	SoyFACE	PHACE
T_{cR}, °C	2.0	2.5	4.7
T_{cH}, °C	2.0	2.7	4.7
$T_{cH} - T_{cR}$, °C	0.4	0.5	0.8
Z, W m^{-2}	168	614	282

especially at night (Fig. 6h; RMSD of 614 W m^{-2}, Table 3). For the predictions, the minimum electrical power was set at 470 W m^{-2}, corresponding to 1/8 of maximum power or 1/4 of the PID control signal (power varies with the square of the voltage), which was programmed into the datalogger. However, in Fig. 6h the minimum measured values appear to be about 750 W m^{-2}. Yet, when this value was used as the minimum power for the predictions, the predicted T_{cH} were much higher than observed (not shown).

One objective of this study was to derive a method to predict the energy requirements for infrared warming of open-field plots for higher degrees of warming. To better account for buoyancy effects than done previously (Kimball, 2005), we adopted the well-accepted MOST for calculating r_a, unless conditions were very stable with low wind, for which the modified American Society of Heating, Refrigerating, and Air-Conditioning Engineers (1972) equation (Eq. [18]) was used. This methodology produced predictions of the T_{cR} of the unheated plot (Fig. 2, 6b, 6f, and 6j), which are the important reference temperatures against which to determine the desired T_{cH} of the heated plot. The setpoint difference for SoyFACE is 3.5°C, the largest for any such experiment reported to date. However, the greater measured amount of required power compared with predicted (Fig. 6h; Table 3) suggests that possibly the r_a was lower than predicted by MOST for the heated plot and/or r_c was lower than the 200 s m^{-1} assumed for unstressed nighttime conditions. On the other hand, the nighttime setpoint differences for Hot Serial Cereal and PHACE were both 3.0°C, which is only slightly less than that for SoyFACE (3.5°C), and the predictions of power requirements were much closer for these two experiments (Tables 2 and 3; Fig. 6d and 6l). Thus, the results were not consistent among the experiments.

The MOST is a one-dimensional theory. It is conceivable that for these 3-m-diameter plots, a more organized three-dimensional flow pattern occurred analogous to the extreme example of the plume of a candle, and therefore a three-dimensional analysis may be needed. It would be desirable to conduct additional experiments with larger degrees of warming to provide a more rigorous test of the methodology presented here to predict the energy requirements for such larger degrees of warming of open-field plots.

CONCLUSIONS

1. For computing the aerodynamic resistance of normal open-field plots from weather data, use of the Mahrt and Ek (1984) formulation to provide the initial conditions for MOST nearly eliminated problems with non-convergence, and it also minimized problems with the dependency of the final solutions for sensible and latent heat fluxes on the initial values used to start the iterations.
2. Under low-wind, stable conditions, use of the American Society of Heating, Refrigerating, and Air-Conditioning Engineers (1972) equation for natural convection from a semi-infinite plane with the coefficient changed from 1.52 to 5.0 to calculate aerodynamic resistance provided good agreement of predicted canopy temperatures of normal open-field plots with measured values.
3. Use of the hybrid Mahrt–Ek with MOST in no. 1 above along with no. 2 above for calm conditions for calculating aerodynamic resistance and following Campbell and Norman (1998) to vary daytime canopy resistance with light and temperature provided good predictions of wheat canopy temperatures in open-field plots most of the time during six growing seasons, as well as for selected weeks of data over soybean and over northern mixed-grass prairie.
4. (a) Using 1–3 above to obtain the canopy temperatures of unheated plots, (b) adding the desired degrees of warming for an experiment, and (c) re-solving the energy balance equation to obtain the amount of additional energy impinging on the canopy from infrared heaters to achieve the canopy temperature of the heated plots proved to be a feasible way to predict the energy requirements for infrared heating of open-field plots at higher degrees of warming than done previously. The method appeared to work most of the time for wheat, soybean, and northern mixed-grass prairie, but additional experiments are warranted to test the procedure at higher degrees of warming than 3.5°C, the highest used in experiments to date.
5. During six growing seasons, the energy requirements of the T-FACE system for raising the canopy temperatures of 3-m-diameter wheat plots by 1.5°C in daytime and 3.0°C at night averaged about 7.0 kWh m^{-2} d^{-1} whether determined from the control signals from the dataloggers or predicted using no. 4 above. However, the power company's meters suggest it could have been about 50% higher.
6. During the six growing seasons, the hexagonal arrays of infrared heaters used in no. 5 above provided degrees of warming such that the modes of the distribution of the warming for day and night were within 0.1°C of the desired setpoint differences, but the distributions were skewed to lower degrees of warming because the capacity of the T-FACE system could not maintain the warming under high wind speeds, so the resultant average degrees of warming were 1.3 and 2.7°C during day and night, respectively.

ACKNOWLEDGMENTS

This research was supported by the USDA–ARS and the University of Arizona. We acknowledge the helpful cooperation of Dr. Robert Roth and his staff at the University of Arizona, Maricopa Agricultural Center, Maricopa, AZ. Technical assistance by Charles Blackshear, Matthew Conley, Steven Farnsworth, Justin Laughridge, Laura Olivieri, and Zahra Troeh is appreciated. Trade names and company names are included for the benefit of the reader and do not imply any endorsement or preferential treatment of the product by the authors, the USDA, or the University of Arizona.

REFERENCES

Allen, R.G., I.A. Walter, R.L. Elliott, T.A. Howell, D. Itenfisu, M.E. Jensen, and R.L. Snyder. 2005. The ASCE standardized reference evapotranspiration equation. Am. Soc. Civ. Eng., Reston, VA.

American Society of Heating, Refrigerating, and Air-Conditioning Engineers. 1972. ASHRAE handbook of fundamentals. ASHRAE, New York.

Aphalo, P.J., and P.G. Jarvis. 1993. An analysis of Ball's empirical model of stomatal conductance. Ann. Bot. 72:321–327. doi:10.1006/anbo.1993.1114

Bernacchi, C.J., B.A. Kimball, D.R. Quarles, S.P. Long, and D.R. Ort. 2007. Decreases in stomatal conductance of soybean under open-air elevation of [CO_2] is closely coupled with decreases in ecosystem evapotranspiration. Plant Physiol. 143:134–144. doi:10.1104/pp.106.089557

Blonquist, J.M., Jr., J.M. Norman, and B. Bugbee. 2009. Automated measurement of canopy stomatal conductance based on infrared temperature. Agric. For. Meteorol. 149:1931–1945. doi:10.1016/j.agrformet.2009.06.021

Campbell, G.S., and J.M. Norman. 1998. An introduction to environmental biophysics. Springer, New York.

Christensen, J.H., B.J. Hewitson, A. Busuioc, A. Chen, X. Gao, I. Held, et al. 2007. Regional climate projections. In: S. Solomon et al., editors, Climate change 2007: The physical science basis. Contribution of Working Group I to the Fourth Assessment Report of the Intergovernmental Panel on Climate Change. Cambridge Univ. Press, Cambridge, UK. p. 847–940.

Collatz, G.J., J.T. Ball, C. Grivet, and J.A. Berry. 1991. Physiological and environmental regulation of stomatal conductance, photosynthesis and transpiration: A model that includes a laminar boundary layer. Agric. For. Meteorol. 54:107–136. doi:10.1016/0168-1923(91)90002-8

Duffie, J.A., and W.A. Beckman. 1974. Solar energy thermal processes. John Wiley & Sons, New York.

Ham, J.M. 2005. Useful equations and tables in micrometeorology. In: J.L. Hatfield, and J.M. Baker, editors, Micrometeorology in agricultural systems. Agron. Monogr. 47. ASA, CSSA, and SSSA, Madison, WI. 533–560. doi:10.2134/agronmonogr47.c23

Harte, J., and R. Shaw. 1995. Shifting dominance within a montane vegetation community: Results of a climate-warming experiment. Science 267:876–880. doi:10.1126/science.267.5199.876

Idso, S.B. 1981a. An experimental determination of the radiative properties and climatic consequences of atmospheric dust under nonduststorm conditions. Atmos. Environ. 15:1251–1259. doi:10.1016/0004-6981(81)90316-4

Idso, S.B. 1981b. A set of equations for full spectrum and 8–14 μm and 10.5–12.5 μm thermal radiation from cloudless skies. Water Resourc. Res. 17:295–304. doi:10.1029/WR017i002p00295

Idso, S.B., R.D. Jackson, W.L. Ehrler, and S.T. Mitchell. 1969. A method for determination of infrared emittance of leaves. Ecology 50:899–902. doi:10.2307/1933705

Jackson, R.D., M.S. Moran, L.W. Gay, and L.H. Raymond. 1987. Evaluating evaporation from field crops using airborne radiometry and ground-based meteorological data. Irrig. Sci. 8:81–90. doi:10.1007/BF00259473

Kaw, A., and E. Kalu. 2008. Numerical methods with applications. Univ. of South Florida, Tampa. http://numericalmethods.eng.usf.edu/topics/textbook_index.html.

Kimball, B.A. 1973. Simulation of the energy balance of a greenhouse. Agric. Meteorol. 11:243–260. doi:10.1016/0002-1571(73)90067-8

Kimball, B.A. 2005. Theory and performance of an infrared heater for ecosystem warming. Global Change Biol. 11:2041–2056. doi:10.1111/j.1365-2486.2005.1028.x

Kimball, B.A. 2011. Comment on the comment by Amthor et al. on "Appropriate experimental ecosystem warming methods" by Aronson and McNulty. Agric. For. Meteorol. 151:420–424. doi:10.1016/j.agrformet.2010.11.013

Kimball, B.A., and M.M. Conley. 2009. Infrared heater arrays for warming field plots scaled up to five meters diameter. Agric. For. Meteorol. 149:721–724. doi:10.1016/j.agrformet.2008.09.015

Kimball, B.A., M.M. Conley, S. Wang, X. Lin, C. Luo, J. Morgan, and D. Smith. 2008. Infrared heater arrays for warming ecosystem field plots. Global Change Biol. 14:309–320. doi:10.1111/j.1365-2486.2007.01486.x

Kimball, B.A., S.B. Idso, and J.K. Aase. 1982. A model of thermal radiation from partly cloudy and overcast skies. Water Resour. Res. 18:931–936. doi:10.1029/WR018i004p00931

Kimball, B.A., R.L. LaMorte, P.J. Pinter, Jr., G.W. Wall, D.J. Hunsaker, F.J. Adamsen, et al. 1999. Free-air CO_2 enrichment (FACE) and soil nitrogen effects on energy balance and evapotranspiration of wheat. Water Resour. Res. 35:1179–1190. doi:10.1029/1998WR900115

Kimball, B.A., R.L. LaMorte, R.S. Seay, P.J. Pinter, Jr., R.R. Rokey, D.J. Hunsaker, et al. 1994. Effects of free-air CO_2 enrichment on energy balance and evapotranspiration of cotton. Agric. For. Meteorol. 70:259–278. doi:10.1016/0168-1923(94)90062-0

Kimball, B.A., J.W. White, G.W. Wall, and M.J. Ottman. 2012. Infrared-warmed and un-warmed wheat vegetation indices coalesce using canopy-temperature-based growing degree days. Agron. J. 104:114–118. doi:10.2134/agronj2011.0144

Lascano, R.J., and C.H.M. van Bavel. 2007. Explicit and recursive calculation of potential and actual evapotranspiration. Agron. J. 99:585–590. doi:10.2134/agronj2006.0159

Mahrt, L., and M. Ek. 1984. The influence of atmospheric stability on potential evapotranspiration. J. Clim. Appl. Meteorol. 23:222–234. doi:10.1175/1520-0450(1984)023<0222:TIOASO>2.0.CO;2

Meehl, G.A., T.F. Stocker, W.D. Collins, P. Friedlingstein, A.T. Gaye, J.M. Gregory, et al. 2007. Global climate projections. In: S. Solomon et al., editors, Climate change 2007: The physical science basis. Contribution of Working Group I to the Fourth Assessment Report of the Intergovernmental Panel on Climate Change. Cambridge Univ. Press, Cambridge, UK. p. 747–845.

Monteith, J.L. 1973. Principles of environmental physics. Edward Arnold, London.

Morgan, J.A., D.R. LeCain, E. Pendall, D.M. Blumenthal, B.A. Kimball, Y. Carrillo, et al. 2011. C_4 grasses prosper as carbon dioxide eliminates desiccation in warmed semi-arid grassland. Nature 476:202–206. doi:10.1038/nature10274

Nijs, I., F. Kockelbergh, H. Teughels, H. Blum, G.H. Hendrey, and I. Impens. 1996. Free air temperature increase (FATI): A new tool to study global warming effects on plants in the field. Plant Cell Environ. 19:495–502. doi:10.1111/j.1365-3040.1996.tb00343.x

Ottman, M.J., B.A. Kimball, J.W. White, and G.W. Wall. 2012. Wheat growth response to increased temperature from varied planting dates and supplemental infrared heating. Agron. J. 104:7–16. doi:10.2134/agronj2011.0212

Prata, A.I. 1996. A new long-wave formula for estimating downward clear-sky radiation at the surface. Q. J. R. Meteorol. Soc. 122:1127–1151. doi:10.1002/qj.49712253306

Prueger, J.H., and W.P. Kustas. 2005. Aerodynamic methods for estimating turbulent fluxes. In: J.L. Hatfield and J.M. Baker, editors, Micrometeorology in agricultural systems. Agron. Monogr. 47. ASA, CSSA, and SSSA, Madison, WI. p. 407–436. doi:10.2134/agronmonogr47.c18

Ruiz-Vera, U.M., M. Siebers, S.B. Gray, D.W. Drag, D.M. Rosenthal, B.A. Kimball, et al. 2013. Global warming can negate the expected CO_2 stimulation in photosynthesis and productivity for soybean grown in the midwestern United States. Plant Physiol. 162:410–423. doi:10.1104/pp.112.211938

Sellers, W.D. 1965. Physical climatology. University of Chicago Press, Chicago.

Spitters, C.J.T., H.A.J.M. Toussaint, and J. Goudriaan. 1986. Separating the diffuse and direct component of global radiation and its implications for modeling canopy photosynthesis: I. Components of incoming radiation. Agric. For. Meteorol. 38:217–229.

Wall, G.W., B.A. Kimball, J.W. White, and M.J. Ottman. 2011. Gas exchange and water relations of spring wheat under full-season infrared warming. Global Change Biol. 17:2113–2133. doi:10.1111/j.1365-2486.2011.02399.x

Wall, G.W., J.E.T. McLain, B.A. Kimball, J.W. White, M.J. Ottman, and R.L. Garcia. 2013. Infrared warming affects intra-row soil carbon dioxide efflux during vegetative growth of spring wheat. Agron. J. 105:607–618. doi:10.2134/agronj2012.0356

White, J.W., B.A. Kimball, G.W. Wall, and M.J. Ottman. 2011. Responses of time of anthesis and maturity to sowing dates and infrared warming in spring wheat. Field Crops Res. 124:213–222. doi:10.1016/j.fcr.2011.06.020

White, J.W., B.A. Kimball, G.W. Wall, and M.J. Ottman. 2012. Cardinal temperatures for wheat leaf appearance as assessed from varied sowing dates and infrared warming. Field Crops Res. 137:213–220. doi:10.1016/j.fcr.2012.08.013